Improvements in Post-Processing of Signals Acquired from a Lamb Wave Based SHM System for Detecting Corrosion in Aluminum

Roger F. LARICO *, Paulo H. de O. LOPES *, Alysson F. MAZONI *,
Bernardo J. G. DE ARAGAO *,+, Edmilson S. SILVA *, Tiago F. A. SANTOS *,
Valdir A. DE ASSIS *
* CPqD, Campinas, Brazil
http://www.cpqd.com.br/en/
+ grbernardo@cpqd.com.br

Abstract. A method was developed for the detection of corrosion by mass loss in aluminum strips using Lamb waves in pitch-catch mode and a signal correlation based technique. This technique compares the measured signals of the damaged structures with that of the undamaged structure. However, this technique does not allow for the detection or differentiation of minor damages by mass loss.

This work presents an refinement of the technique that improves the ability to distinguish between damages of small mass loss. It includes the following features: Choice of the best excitation frequency and of the best wavelet decomposition, calculus of the best window in time to distinguish between damaged and undamaged states and of the best metric to assess damage condition (Correlation, Mahalanobis distance and Minkowski distance).

Six aluminum strips 914 mm by 14 mm by 1.6 mm were tested. The characteristics of the excitation signal were as follows: 7 count sine burst with Hanning window, amplitude of 5V and frequency of 100 kHz. Signal generation and recording was carried out with a PXI platform of National Instruments. Simulated holes of increasing depths were obtained by electrochemical polishing.

The results obtained so far showed that the POD â vs. a curve is strongly affected by the metric chosen. The $a_{90/95}$ value using correlation is around 0.3 mm, whereas using Mahalanobis distance is half that value (0.1594 mm).

Further developments of the technique includes the extension of the technique to aluminum sheet, including damage localization and POD analysis.

Introduction

Corrosion is a major cause to ground an airplane, reducing its availability and increasing its maintenance cost. Therefore, several structural health monitoring (SHM) techniques have arisen in the last decades that allow for the early detection of corrosion damage. Among them are those based on guided waves which use of piezoelectric wafer active sensors (PWAS) bonded to the structure to be monitored for corrosion.

Corrosion damage results in a local thickness reduction of the aluminum of the airplane's fuselage which can pose a threat to the plane's structural integrity. The capability of the SHM system to detect corrosion has to be assessed for its probability of detection (POD) as a function of damage size [1].

A method was developed for the detection of corrosion by mass loss in aluminum strips using Lamb waves in pitch-catch mode and a signal correlation based technique, by which the measured signals of the damaged structures were compared with that of the undamaged structure. Damaged structures were obtained through the introduction of artificial defects of increasing depths by electrolytic polishing [2]. According to Lamb wave theory, symmetric (S0) and antisymmetric (A0) waves can be generated in a broad range of signal excitation frequencies, whose propagation velocity depends on the frequency and the thickness of the structural element (strips, sheets) [3].

However, this technique originally did not allow for the detection or differentiation of minor damages by mass loss (low depths defects). The POD â (response) vs. a (depth) curve obtained resulted in $a_{90/95}$ value of 0.30 mm.

A refinement of the technique is presented in this paper which improves the ability to distinguish between damages of low depths. This was accomplished through different ways, as described below.

1.1 Window in time.

The first signal packets recorded are those due to the S0 and A0 waves. It is important to isolate these waves from the rest of the signal to investigate how their propagation velocity is affected by the damage (see Fig. 1).

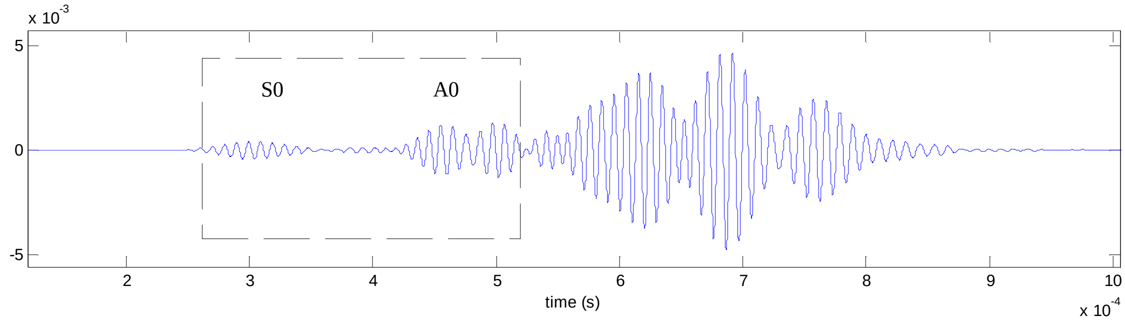

Fig. 1. S0 and A0 waves in recorded signal (y-axis is signal amplitude in A) with frequency 100 kHz.

1.2 Choice of the best excitation frequency.

For a frequency range of 0 to 0.4 MHz, very common in SHM systems [3], the group velocity diagram of Fig. 2 for aluminium shows that, for a thickness value of 2 mm, the best frequency range lies in the 0.10 MHz to 0.15 MHz (0.2 to 0.3 MHz×mm), since in this

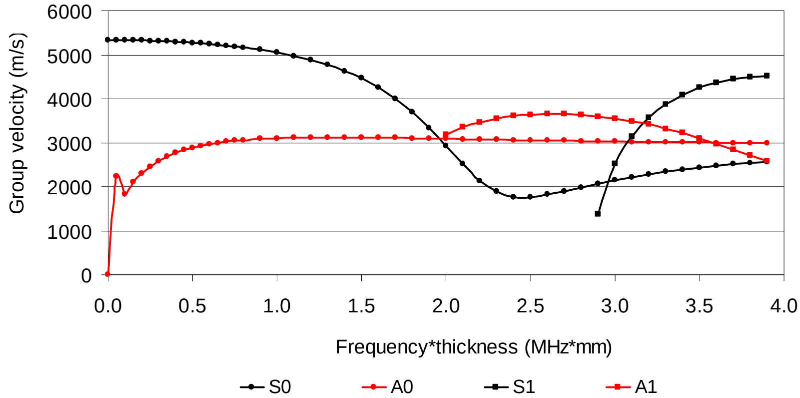

Fig. 2. Group velocity diagram for aluminum.

range the A0 waves will experience a velocity decrease with decrease in thickness (increase in damage depth). The larger the damage depth, the more significant will be the velocity decrease. S0 waves propagation velocity will be less affected by thickness reduction in this frequency range.

1.3 Choice of the best wavelet decomposition.

Wavelet transform has been used in variety of engineering applications. As was described in [4], some of key features of wavelet transform which make it such an useful tool are as follows: spatial-frequency localization, energy compaction, decaying magnitude of wavelet coefficients across sub-bands [5]–[7]. The DWT of a signal x is calculated by passing it through a series of filters in one, two or more dimension. In order to perform this transformation the original signal is passed through a band-pass filter (called by *G* and is named mother wavelet) to give a detail component for the first level. At the same level, convolving the signal with a low-pass filter (called by *H*) brings another component named approximate due to its low resolution. *G* and *H* are orthogonal vectors with N×1 elements [4], [8]. This procedure is shown in Fig. 3.

An advantage (app detect flaws) is that the main components of the source wave signal are focused in detailed parts of level 6 (d6) [9] or level 7 (d6) [5], [10]. Mother-wavelet used in the wavelet decomposition belong to the families symlet, coiflet, daubechies, etc.

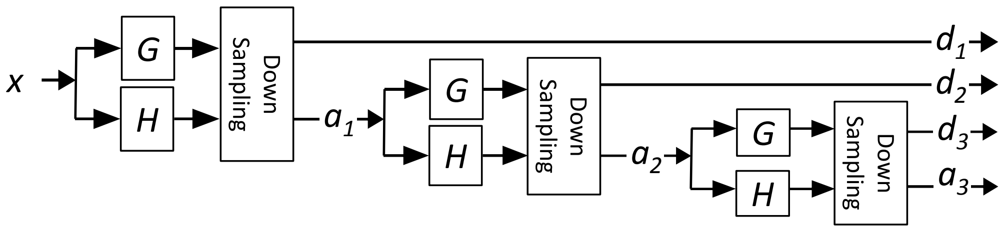

Fig. 3. Decomposition of original signal X by DWT [11].

1.4 Choice of similarity metric for baseline and outlier signals.

Three metrics were investigated:

1.4.1 Correlation coefficient.

The general principle is that a measure of similarity should be invariant under admissible data transformations, which is to say changes in scale. Thus, it is a measure designed for interval data. The correlation coefficient, automatically disregards differences in variables that can be attributed to differences in scale. The sample correlation coefficient is given by Equation (1):

$$r_{xy} = \frac{\sum_i (x_i - \bar{x})(y_i - \bar{y})}{\sqrt{\sum_i (x_i - \bar{x})^2 \sum_i (x_i - \bar{y})^2}} \qquad (1)$$

where $\bar{x}$ and $\bar{y}$ are the sample means of x and y, which refers to the undamaged and damaged state, respectively. In this work, the similarity metric used in fact is 1-r_{xy}, in order to have an increasing curve, similar to the other metrics.

1.4.2 Mahalanobis distance.

This metric is defined from the definition of multivariate normal distribution [12]. The estimator of the Mahalanobis distance between a potential outlier vector y (damaged state) and baseline sample (undamaged state) set can be obtained by Equation (2):

$$D_{xy}^2 = (y - \bar{x})\ \Sigma^{-1}\ (y - \bar{x})' \qquad (2)$$

where $\bar{x}$ is the average of the baseline sample feature vectors, and Σ the estimated covariance matrix. When the structural system is damaged, it is expected that the Mahalanobis distance of vectors will increase significantly [13].

1.4.3 Minkowski distance of degree three.

This metric can be considered a generalization of Euclidian distance (p=3) and is given by Equation (3).

$$m_{xy} = \left(\sum_i (x_i - y_i)^p \right)^{\frac{1}{p}} \qquad (3)$$

The proposed refinement of the method is obtained by searching for the parameters which present linear regression with higher coefficient of determination for the behaviour of the system and also in analysis of the confidence interval. This amounts to a linear correspondence from damage to detection (POD guided research).

Experimental setup

Aluminum strips 914 mm long by 14 mm wide by 2 mm thick were tested with the configuration of Fig. 4. The PAWS (7mm × 7mm × 0.2 mm) were attached with epoxy resin [3]. Later, the strips were etched halfway between the sensors to achieve perforation with 10 mm diameter and depths from 0.02mm up to 0.5mm. To operate the system were

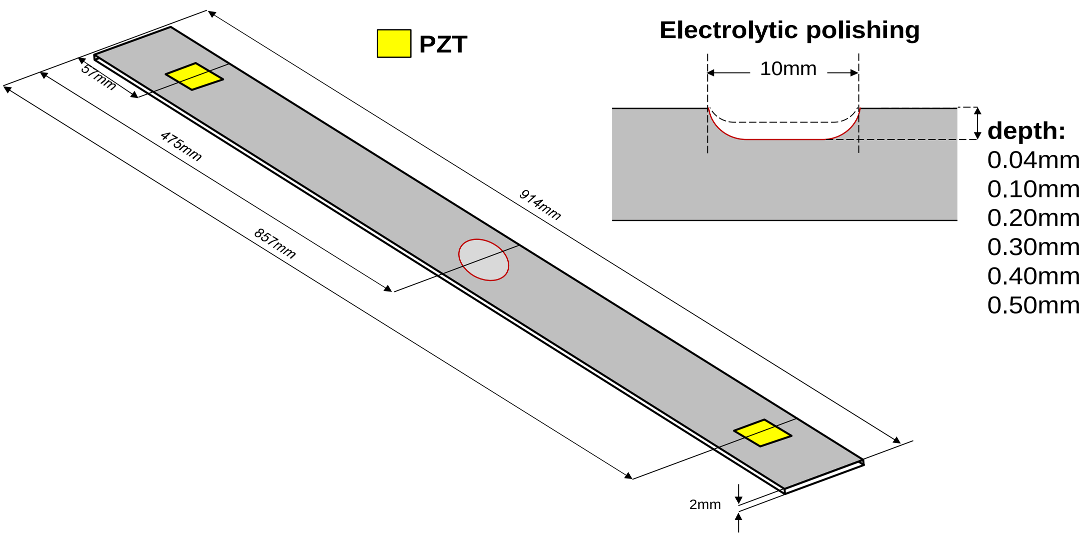

Fig. 4. Configuration of the tested aluminum strips.

developed in LabView applications that generate Hanning signals. Response signals are post processed using Matlab® to find the best parameters and software package ML1823 [1], [14] to perform the calculation of the POD.

Etching was done by electrolytic polishing using a solution composed of 800 ml etanol, 140 ml distilled water and 60 ml of perchloric acid. The electrolytic polishing parameters were: voltage 5V, current 0.2-0.3A and polishing times up to one hour, according to depth.

Lamb waves were generated and recorded in pitch catch mode. The characteristics of the excitation signal were as follows: 7 count sine burst with Hanning window, amplitude of 5V and frequency of 100 kHz (0.1 MHz) and 150 kHz (0.15 MHz). Signal generation and recording was carried out with a NI PXI 5422 platform of National Instruments.

Results

The responses of all samples are simultaneously used in the determination of a linear regression line of the type $y = \alpha + \beta x$, relating damage size with each similarity metric. Thus a particular set of parameters is chosen as best fit for each metric.

- In the case of the correlation coefficient metric, the best set of parameters was using 100 kHz with 7 cycles, mother-wavelet Symlet2 in the interval from 0.33 ms to 0.56 ms.
- In the case of the Mahalanobis distance, the best set of parameters was using 100 kHz with 7 cycles, mother-wavelet Coiflet2 in the interval from 0.323 ms to 0.575 ms.
- Finally, in the case of the Minkowski distance, the best set of parameters was using 100 kHz with 7 cycles, mother-wavelet Symlet2 in the interval from 0.2 ms to 0.575 ms.

For each of these three set configurations are compared the critical points in order to evaluate the best strategy in what concerns false positive results, better sensitivity to smaller damage, confidence bounds. The figures below present the linear regressions of the system data to the left and the POD curve to the right. The surrounding dotted lines get closer to each other at the beginning (smaller damage) until they converge to the point of zero damage. This convergence at the start indicates no false positive results.

The Fig. 5 presents the POD curve that was obtained without any improvement,

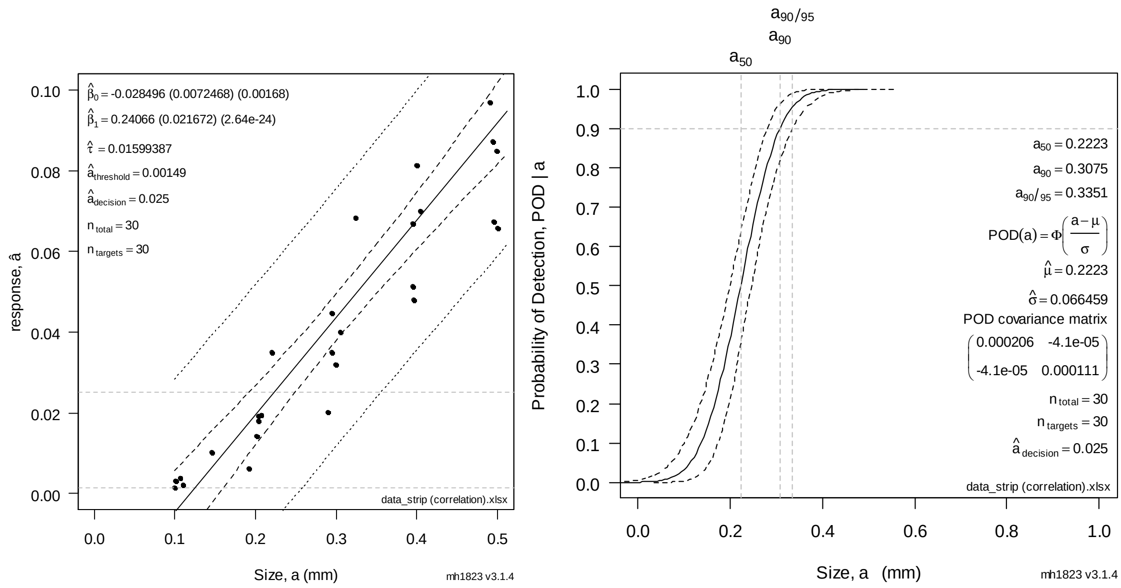

Fig. 5. Curve POD *â vs a* using correlation metric (without improvement).

using correlation coefficient as the similarity metric without Wavelet transform. It can be noticed that the $a_{90/95}$ value, associated to smaller damage for which there is 90% of probability and 95% of confidence bound, is 0.3351 mm.

The Fig. 6 presents the POD curve obtained using the correlation coefficient as the similarity metric and the Wavelet transform with mother-wavelet Coiflet2, in which case $a_{90/95}$ was 0.2382 mm.

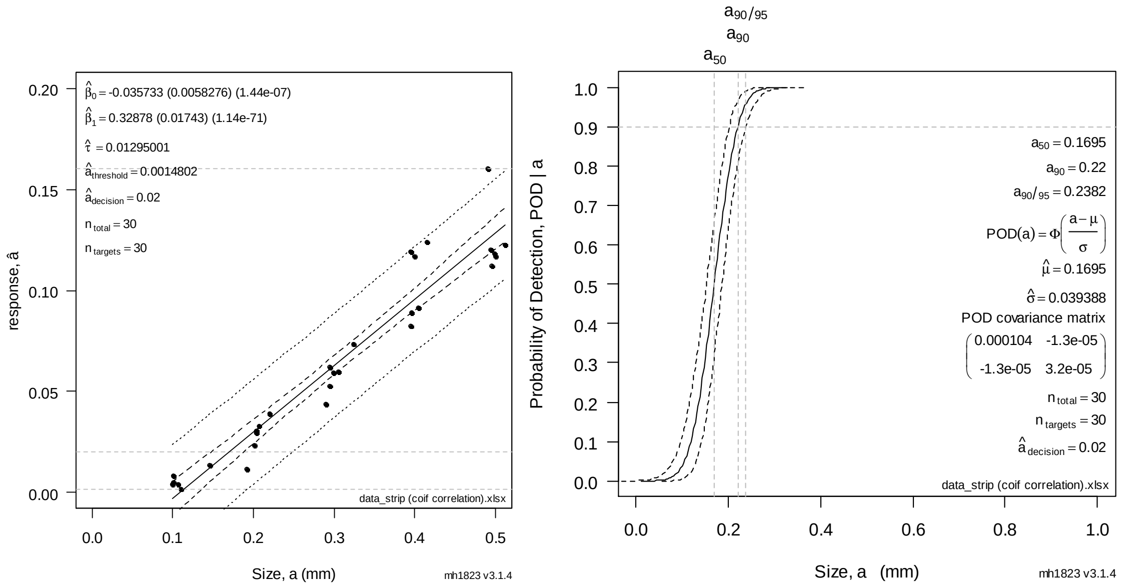

Fig. 6. Curve POD *â vs a* using correlation metric with filter coiflet2 wavelet.

Finally, Fig. 7 presents the improved system. It shows the POD curve obtained using Mahalanobis distance as the similarity metric and mother-wavelet Coiflet2. In this case, $a_{90/95}$ was 0.161 mm.

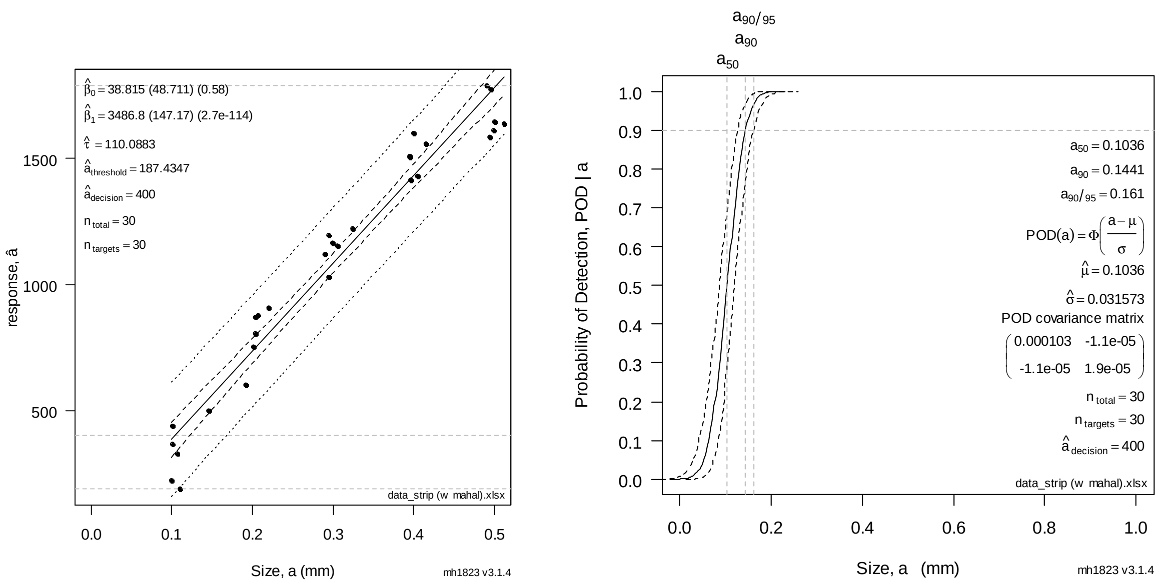

Fig. 7. Curve POD *â vs a* using Mahalanobis metric with filter coiflet2 wavelet (with improvement).

Fig. 8 compares the POD curves without and with improvement, highlighting the decrease in the $a_{90/95}$ value achieved.

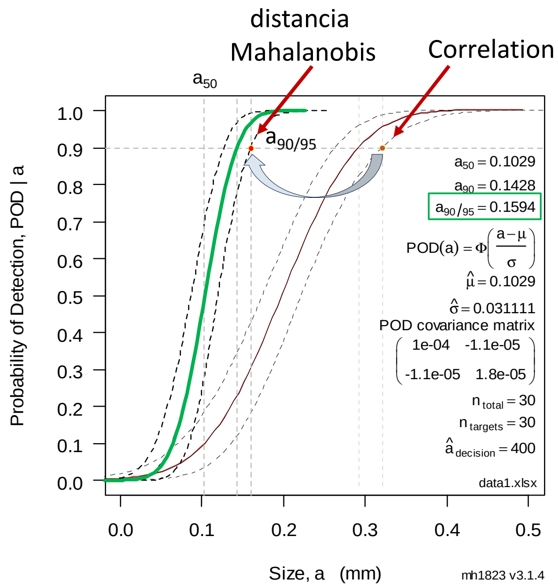

Fig. 8. Comparison between POD *â vs a* without and with improvement.

To obtain these results were tested different combinations of parameters: window in time (between 0.18 ms and 0.73 ms); wavelet families (symlet, coiflet and daubechies,) and Similarity metric (correlation, Mahalanobis, Minkowski distance). In the case of using the distance Minkowski/symlet2 the result is $a_{90/95}$ = 0.25 and in other cases also showed no improvement in relation to Mahalanobis/coiflet2.

Conclusion

The search parameters proved useful to improve the performance of the fault detection capability by the process described. The set of parameters with Mahalanobis distance found for significantly improves the smallest damage that can be detected with a probability of detection 90% and 95% of confidence bound. Applying post processing improvements, the statistical value $a_{90/95}$ = 0.33 mm decreased to $a_{90/95}$ = 0.16 mm, increasing the sensitivity of the system.

References

[1] Department of Defense NDTI/DOD, *Handbook Nondestructive Evaluation System Reability Assessment*, no. April. 2009, pp. 1–160.

[2] P. Silva, B. Aragao, P. Lopes, E. Silva, T. Santos, V. Assis, G. Vasconcelos, M. Hurtado, and A. Mazoni, “Critical issues affecting the performance of PWAS based SHM systems for Corrosion Detection of Aluminum Structures,” in *A Roadmap to Intelligent Structures. Proceedings of the 9th International Workshop on Structural Health Monitoring*, 2003, pp. 1302–1309.

[3] V. Giurgiutiu, *Structural Health Monitoring*, 1st ed. Academic Press, 2007, p. 760.

[4] S. Mallat, *A Wavelet Tour of Signal Processing*. 1999.

[5] P. Souza and E. Nobrega, “A fault location method using Lamb waves and discrete wavelet transform,” *J. Brazilian Soc. Mech. Sci. Eng.*, vol. XXXIV, no. 4, pp. 515–524, 2012.

[6] G. Peng, S. Yuan, and Y.-D. Xu, “Damage Location of two-dimensional structure Based on Wavelet Transform and Active Monitoring Technology of Lamb Wave PENG,” in *Nondestructive Evaluation and Health Monitoring of Aerospace Materials and Composites III*, 2004, vol. 5393, pp. 151–160.

[7] D. Waltisberg and R. Raišutis, “Group velocity estimation of Lamb waves based on the wavelet transform,” *Ultragarsas (Ultrasound)*, vol. 63, no. 4, pp. 35–40, 2008.

[8] “MathWorks - MATLAB and Simulink for Technical Computing.” [Online]. Available: http://www.mathworks.com/.

[9] Y. Lu, L. Ye, and Z. Su, “Crack identification in aluminium plates using Lamb wave signals of a PZT sensor network,” *Smart Mater. Struct.*, vol. 15, no. 3, pp. 839–849, Jun. 2006.

[10] P. Souza and E. Nobrega, “Método para detecção de trincas em vigas utilizando onda de Lamb e a transformada wavelet discreta,” *labplan.ufsc.br*, pp. 1101–1106, 2010.

[11] S. Shahrtash and F. Haghjoo, “Instantaneous wavelet transform decomposition filter for on-line applications,” *Iran. J. Sci. Technol. Trans. Electr. Eng.*, vol. 33, pp. 491–510, 2009.

[12] P. Mahalanobis, “On the generalized distance in statistics,” *Proc. Natl. Inst. Sci. India*, vol. 2, pp. 49–55, 1936.

[13] R. Yao and S. Pakzad, “Statistical modeling methods for structural damage identification,” *6th Int. Work. Adv. Smart Mater. Smart Struct. Technol.*, 2011.

[14] C. Annis, “MIL-HDBK-1823A Nondestructive Evaluation System Reliability Assessment.” StatisticalEngineering.com, 2009.

Acknowledgements

The authors express their gratitude to EMBRAER for the authorization to publish this paper. Gratitude is owed also to EMBRAER and FINEP for financial support to carry out the research work related to this paper. Moreover, the coauthors Roger F. Larico and Alysson F. Mazzoni want to thank CNPq for the fellowships which supported their contributions to this research work. Last, but not least, the authors are also thankful to Charles Annis for providing the mh1823POD software package.